NASA Technical Memorandum 83613

Effect of a Rotor Wake on Heat Transfer from a Circular Cylinder

Robert J. Simoneau, Kim A. Morehouse, G. James VanFossen, and Frank P. Behning
Lewis Research Center
Cleveland, Ohio

Prepared for the
Twenty-second National Heat Transfer Conference
cosponsored by the ASME and AIChE
Niagara Falls, New York, August 5–8, 1984

NASA

ENTER:
21 1 1 RN/NASA-TM-83613
DISPLAY 21/2/1
84N21832*# ISSUE 12 PAGE 1815 CATEGORY 34 RPT#: NASA-TM-83613
E-2039 NAS 1.15:83613 84/08/08 18 PAGES UNCLASSIFIED DOCUMENT
UTTL: Effect of a rotor wake on heat transfer from a circular cylinder
AUTH: A/SIMONEAU, R. J.; B/MOREHOUSE, K. A.; C/VANFOSSEN, G. J.; D/BEHNING, F. P.
CORP: National Aeronautics and Space Administration, Lewis Research Center, Cleveland, Ohio. AVAIL.NTIS SAP: HC A02/MF A01
Proposed for presentation at 22nd Natl. Heat Transfer Conf., New York, 5-8 Aug. 1984; sponsored by ASME and AIChE
MAJS: /*AIRFOILS/*CIRCULAR CYLINDERS/*HEAT TRANSFER/*ROTOR BLADES (TURBOMACHINERY)/*TURBULENT FLOW
MINS: / PRESSURE EFFECTS/ REYNOLDS NUMBER/ STATORS/ THERMAL CONDUCTIVITY/ VORTICES/ WIND TUNNEL TESTS
APA: Author
ABS: The effect of a rotor wake on heat transfer to a downstream stator was investigated. The rotor was modeled with a spoked wheel of 24 circular pins 1.59 mm in diameter. One of the stator pins was electrically heated in the midspan region and circumferentially averaged heat transfer coefficients were obtained. The experiment was run in an annular flow wind tunnel using air at ambient temperature and pressure. Reynolds numbers based on stator cylinder diameter ranged from .001 to .00001. Rotor blade passing frequencies ranged from zero to 2500 Hz. Stationary grids were
ENTER:

EFFECT OF A ROTOR WAKE ON HEAT TRANSFER FROM A CIRCULAR CYLINDER

Robert J. Simoneau, Kim A. Morehouse, G. James VanFossen,
and Frank P. Behning

National Aeronautics and Space Administration
Lewis Research Center
Cleveland, Ohio 44135

E-2039

ABSTRACT

An experiment has been conducted to scope the effect of a rotor wake on heat transfer to a downstream stator. The rotor was modeled with a spoked wheel of 24 circular pins 1.59 mm in diameter. The stator was also modeled with a spoked wheel of 8 circular pins 12.7 mm in diameter. One of the stator pins was electrically heated in the midspan region and circumferentially averaged heat transfer coefficients were obtained. The experiment was run in an annular flow wind tunnel using air at ambient temperature and pressure. Reynolds numbers based on stator cylinder diameter ranged from 10^4 to 10^5. Rotor blade passing frequencies ranged from zero to 2500 Hz. Stationary grids were used to vary the rotor inlet turbulence from one to four percent. The rotor-stator spacings were one and two stator pin diameters. In addition to the heat transfer coefficients, turbulence spectra and ensemble averaged wake profiles were measured.

At the higher Reynolds numbers, which is the primary range of interest for turbine heat transfer, the rotor wakes increased Nusselt number from 10 to 45 percent depending on conditions. At lower Reynolds numbers the effect was as much as a factor of two. The rotor wake effect appeared to overpower and wash out the inlet turbulence effect. By treating the rotor wakes as turbulence intensity, a first order correlation could be obtained.

NOMENCLATURE

A	area, m^2
BPF	blade passing frequency, Hz
D	stator pin diameter, m
E	voltage, volts
f	frequency, Hz
I	current, amps
k	thermal conductivity, W/m K
Nu	Nusselt number (eq. (1))
Pr	Prandtl number (0.71 for air)
Q	power, W
r	recovery factor
Re	Reynolds number (eq. (3))
S	Strouhal number (eq. (4))
T	temperature, K
Tu	turbulence intensity, U_{rms}/U_m
U	mass averaged velocity, m/s
w	mass flow rate, kg/s
τ	time constant, s
μ	viscosity, N/s m^2

Subscripts

avg	average
aw	adiabatic wall conditions
chn	channel
cyl	cylinder
l	loss
m	mean
o	stagnation conditions
rms	root mean square
s	static conditions
w	wall conditions

INTRODUCTION

One of the most critical heat transfer areas on a turbine airfoil is the blunt leading edge. The thin boundary layers associated with stagnation regions are natural high heat transfer areas. The situation is aggravated by the highly disturbed flows associated with turbomachinery. Colladay (1) points out that turbine airfoil leading edges are normally circular in cross section and that conventional design practice is to apply an augmentation factor of 1.2 to 1.8 to empirical correlations for flow over cylinders. Because many important heat transfer problems are associated with cylinders in crossflow, heat transfer to circular cylinders has been an extensively explored research area. Surveys by Kestin (2) and Zukauskas (3) are but two sources of the body of research. Despite extensive research, Morkovin (4) points out that the study of flow about circular cylinders is far from achieving fundamental understanding.

The present paper is one part of a program at the Lewis Research Center designed to systematically investigate the mechanisms associated with this important heat transfer phenomenon. The program at Lewis has two main thrusts. The first is to examine in careful detail the heat transfer mechanisms associated with turbulence in the stagnation region of cylinders. The second is to establish an experiment which simulates a rotor wake environment in which heat transfer data can be measured. The present work is part of the latter thrust. The experiment simulates the stator with a circular cylinder with a splitter plate behind it. The wakes are created by rotating a spoked wheel, also of circular cylinders, in front of it. This technique for producing wakes has been used before in turbomachinery research (5, 6) and seems to work quite well.

The present paper describes in detail an experiment which produces the conditions of a simulated stator in a rotor wake. It examines the flow field created by the experiment, including the wake profiles and spectra. It presents circumferentially averaged heat transfer data, both with and without the rotor, and over a range of inlet turbulence intensity from one to four percent. The blade passing frequencies are from 500 to 2500 Hz. This is low relative to turbomachinery, but high enough to identify wake effects. The Reynolds number range, based on the stator cylinder diameter, is from 10^4 to 10^5, which is typical of turbines.

DESCRIPTION OF EXPERIMENT

The general concept of the rotor wake experiment is illustrated in Fig. 1. The flow passage was annular in cross section. The flow passed over a rotor of circular pins, creating a wake, which then impinged on the circular pin stator. The wakes were produced by rotating a wheel of 24 pins, 1.6 mm diameter by 68.0 mm long, upstream of the heated stator. The spacing between the rotor and stator could be varied. Spacings of 12.7 and 25.4 mm (one and two stator pin diameters) were selected. The rotor speed was continously variable from 500 to 7300 rpm. Speeds corresponding to blade passing frequencies (BPF) of 500, 1500, and 2500 Hz were selected for this experiment. The stator contained eight equispaced pins, 12.7 mm diameter by 68.0 mm long. Each pin had a 1.6 mm thick splitter plate behind it to eliminate the oscillations associated with the alternately shedding vorticies. One of the eight stator pins was heated. The details of the heated pin are shown in Fig. 2(a). The heated pin was made by winding a resistance heating wire around a mandrel epoxied inside a heavy wall copper tube. Only the center one half of the span of the pin was heated. Eight chromel-constantan, Type E, thermocouples were placed at equal distance around the circumference at the mid-span. Because of the heavy copper walls, the heat transfer coefficients measured were average values, both circumferentially and spanwise, over the midspan region of the pin.

This package was installed in a vertically oriented annular flow wind tunnel, shown in Fig. 2(b), which was operated at abient temperature and pressure. The test section annulus was 40.64 cm O.D. by 27.05 cm I.D. The inlet to the tunnel had a calming section which contained an 18 mesh screen, a honeycomb of plastic soda straws (6.4 mm I.D. by 184 mm long), and a second 18 mesh screen. The terminology 18-mesh means 18 wires to the inch in a square pattern. The flow was then accelerated by contracting the outer wall (shroud) of the annulus through an elliptical contraction, changing the area by 8.3 to 1. The contraction was designed using the program described in Ref. 7. The centerbody was constant diameter through the whole flow passage. The centerbody, which did not rotate, contained a bearing and through this bearing was supported on the shaft of the rotor. It was maintained in lateral alignment by the screen and soda straw assembly. There were no upstream struts. The turbulence generating grids were made of interwoven wire mesh. Four grids of 3, 5, 10, and 18-mesh size, as well as no grid were used. The grid wire diameters were 1.60, 1.04, 0.51, and 0.23 mm, respectively. Since the grids had a square pattern and were installed in an axisymmetric flow passage, the pattern changed circumferentially. This appeared to be significant only for the coarsest grid. The section of the tunnel from the end of the inlet to the stator was made of a set of interchangeable rings, thus the grids could be moved to various axial positions. For the present tests they were always located 19.7 cm upstream of the stator, the furthest position.

The rotor was mounted in a fixed axial position. The rotor-stator spacing was achieved by moving the stator ring. The rotor pins were removeable from the disk, allowing variations in size and number up to a maximum of 24. For the present experiment all tests were run with 24 pins, 1.6 mm diameter. The rotor was driven externally, as shown in Fig. 2, using a variable speed D.C. motor and a belt and pulley arrangement. The control was excellent and the speed could be varied from about 500 to 7300 rpm (BPF: 200 to 2920 Hz). The motor could be run both forward and reverse.

Immediately downstream of the rotor-stator assembly were a set of flow straighteners, approximately 46 cm long, to minimize any upstream swirling effects produced by the downstream turning. After the turn the flow passed through flow straighteners and a sharp-edged orifice, designed according to ASME standards (8). The flow was then exhausted through a throttleable butterfly valve into the laboratory altitude exhaust system at a pressure of approximately 34 kPa.

The essential instrumentation is shown on Fig. 2. These include the measurements necessary to determine Nusselt number, Reynolds number, blade passing frequency, turbulence intensity, and wake velocity profiles. The Nusselt numbers presented herein are a circumferential average over the midspan region of the stator pin as shown on Fig. 2(a). The heat flux was determined by measuring the voltage and current to the resistance heater buried in the cylinder and the wall temperature was determined by averaging the eight thermocouples. An in-situ calibration for conduction heat losses was conducted and a correction was included in the data reduction. The resulting equation was:

$$Nu = \frac{D[(EI) - Q_l]}{k\,[T_{w,avg} - T_{aw}]\,A_{cyl}} \qquad (1)$$

The free stream reference temperature was taken as the adiabatic wall temperature, according to the recommendation of Eckert (9) and computed as follows:

$$T_{aw} = T_s + r(T_o - T_s) \qquad (2)$$

The recovery factor (r) was assumed to be $\sqrt{Pr}$. The stagnation temperature was determined by

averaging four thermocouples equispaced around the lip of the inlet bellmouth. The static temperature was computed from the compressible flow equations.

Based on earlier work (10), the authors consider the average velocity based on the unobstructed channel to be the appropriate choice in computing the cylinder Reynolds number.

$$Re = \frac{wD}{\mu A_{chn}} \qquad (3)$$

The mass flow rate was computed from the static pressure drop in the inlet contraction. The sharp-edged orifice was used as a backup. The orifice was located in a 46 cm pipe, which was too large for calibration; thus the coefficients were determined from ASME standards (8). The density was computed using the ideal gas equation of state and the transport properties were simple curve fits to the data in Ref. 11.

In addition to the mass-averaged velocity, direct velocity measurements were also made, using both a pitot-static probe and hot wire anemometers. The pitot-static probe was a conventional coaxial probe, 1.6 mm diameter, with a spherical tip and static taps 6 diameters from the tip. This probe and one of the hot wires were installed midway between the turbulence grid and the stator row, as shown on Fig. 2(b). They could be traversed radially. The hot wires were conventional, 6 μm diameter, tungsten single wire probes. The one in the same plane as the pitot-static probe had the wire aligned normal to the channel radius. A second, hook shaped, probe was installed in a fixed position in the stator plane midway across the channel with the wire parallel to a radial line. It was located 15° circumferentially from a stator pin. The hot wires were calibrated and linearized, using a free jet, prior to each run. The maximum velocity of the jet was 106 m/sec. Flow angles were measured with a wedge-shaped pressure probe with a port on each face of the wedge. Pressure differential was measured across the ports and the angle was determined by rotating the probe to a null position.

The rotor speed was measured with a fiber optic sensor sighted onto the tip of the rotor pins. One pin tip was painted white and the rest were blackened. In addition, the speed was also measured with a 60-tooth gear and magnetic sensor mounted at the end of the shaft. All pressures were measured with individual conventional strain gage transducers which had been calibrated in a standards lab. All temperatures were measured with chromel-constantan (Type E) thermocouples except for the reference junction temperature, which was measured with a platinum resistance thermometer.

All the steady state heat transfer and flow data were recorded on the laboratory central data acquistion/minicomputer system, known as ESCORT II (12), which provided real time updates at approximately two second intervals on a CRT. The data were subsequently transmitted to a large central computer for further processing. The hot wire data were recorded in two ways. First, the signals were fed in parallel into an integrating dc voltmeter and an rms voltmeter, both set on a 3-second time constant. The output of these meters was then transmitted as steady state mean and rms velocities to the ESCORT system. The hot wire output was also recorded on a dual channel FFT (Fast Fourier Transform) spectrum analyzer with the once/rev signal on one of the channels, as a trigger source for ensemble averaging.

All of the measurements and computed parameters were analyzed for uncertainty by the methods of Kline and McClintok (13). This was part of the data reduction program and appeared with all output. The uncertainties associated with the key parameters are summarized in the following table. Note that the uncertainties of some parameters vary substantially over the range of the experiment.

Experimental Reynold Number	UNCERTAINTY OF MEASURED VALUES (IN PERCENT)					
	Velocity (pitot-static)	Velocity (hot-wire)	Re	BPF	Tu	Nu
10 000	32.0	2.0	27.8	0.3	1.0	2.5
20 000	7.5	2.1	6.9	↓	↓	↓
50 000	1.5	1.9	2.0			
105 000	.3	3.1	.4			

A few additional comments are necessary. The results are being presented herein with BPF as a parameter, thus in addition to measurement uncertainty it is necessary to state the precision with which points were set. Including the measurement uncertainty, the nominal values of BPF presented herein are within ±1.1 percent of the true value. Although the hot wires were repeatedly calibrated to a relatively low uncertainty, the experience with running the rig suggests higher errors. During each run the hot wires would tend to drift away from the pitot-static probe, sometimes by as much as 26 percent. The pitot-static probe was always in good agreement with mass averaged velocity. This discrepency seemed to increase with running time and was worse at high velocities, especially when extrapolated beyond calibration. Attempts to isolate the problem were never successful, although probe contamination was suspected. Since the hot wire output was almost always used in a relative manner, such as turbulence intensity, the results were still considered valid. However, the uncertainty in the variable Tu is almost surely higher than the analysis indicates, and the absolute values of the hot wire velocity are suspect. The wake shape and spectra measurements should be completely unaffected.

RESULTS AND DISCUSSION

No Rotor Data

A series of tests were run with the rotor removed from the rig in order to establish a reference set of data without the rotor wake effect. A wooden disk was used in place of the rotor to fill the gap.

During this period cross channel velocity surveys were routinely made at the location 9.5 cm upstream of the stator leading edge with both the hot wire and pitot-static probes. Figure 3, taken with no turbulence generating grid in the inlet, is a typical example. The hot wire mean and rms velocity signals were fed into a two pen X-Y plotter with the actuator position output signal driving the x-motion. For these traces the voltmeter time constants were set at 0.1 second, so that disturbances would not be damped out. Figure 3 is a direct reproduction of those plots. The pitot-static probe was traversed in discrete steps and the results subsequently plotted on the same traces. The probes were always traversed in both directions across the channel. In addition, one hot wire point was taken at midchannel on a three second time constant and is plotted on Fig. 3. The mass averaged velocity during the traverse was 61.9 m/s. The pitot-static measured velocity on the channel center-line was 63.0 m/s. The hot wire measured velocity on the center-line (τ = 3 sec) was 64.6 m/s with a turbulence intensity of 0.87 percent. The pitot-static surveys indicated the velocity profile at this station was flat over 89 percent of the channel. The hot wire mean velocity output showed a four percent drop beginning at approximately 2/3 the way across the channel on the shroud side. At approximately the same position the rms velocity rose rapidly to about twice the value near the hub. An extensive series of trial and error tests to isolate the source of this phenomenon were unsuccessful and led ultimately to the conclusion that there was a fundamental flaw in the inlet design. Apparently a small overspeed and separation bubble must have occurred near where the inlet contour transitioned to the straight section. The phenomenon persisted with the smaller (18 and 10 mesh) grids in place. With the larger (5 and 3 mesh) grids in place the phenomenon was washed out. However, with the larger grids the wakes from the grid wires began to appear in both the pitot-static and hot wire signals. For the 3 mesh grid the depth of the wakes at this survey station was about four percent of the mean velocity. These types of hot wire traverses were also taken at nominal velocities of 30, 90, 120 m/s, as well as 60 m/s. The profile shapes were somewhat different but the general results were the same. The non-uniformity in the rms profile was not believed to have a serious effect on the midspan cylinder heat transfer. The only effect, if any, would be at the lowest turbulence levels.

In addition, during these tests the power spectra from the hot wires were frequently measured with the FFT analyzer and plotted with a digital plotter. Both the hot wire outputs at the plane shown in the Fig. 3 data and in the stator plane were examined. The probe was normally on the channel center line. Figure 4 is an example of such output in the stator plane at the high and low grid turbulence levels. The spike in the spectra was almost always present in both hot wire signals at the lower turbulence levels over the entire velocity range. The spike tended to disappear at the higher turbulence. These spikes were examined in terms of Strouhal number based on stator diameter and mass averaged velocity, defined as:

$$S = \frac{fD}{U} \tag{4}$$

For the conditions of Fig. 4 the Strouhal number associated with the frequency of the spike is 0.25. This number suggests that the spike is associated with the vortex shedding from the stator pins. According to Blevins (14) the Strouhal number for a cylinder in the Reynolds number range of the present experiment should be about 0.20. He presents a variety of shapes in crossflow, but none resembling a cylinder with a splitter plate, as used herein. The closest, a bluff body with a tapered afterbody, had a Strouhal number of 0.27.

The heat transfer data acquired without the rotor in place are summarized in Fig. 5. The legend gives the average turbulence level over the Reynolds number range at the two probing stations. At the higher Reynolds number level (Re = 10^5) the data in Fig. 5 agree well with data presented by Kreith (15) and also with earlier work by the authors (10) on a cylinder three diameters long in a rectangular channel. At the lower Reynolds numbers (Re = $2x10^4$) the present data fall between the two referenced sets of data (10 and 15). The majority of the data were taken with the wall temperature at 60° to 65° C. A few points were taken at wall temperatures greater than 75° C, and a few less than 50° C. These addition points were primarily at Reynolds numbers of 25 000; 50 000; 75 000 and 100 000. At the low Reynolds number the data showed little effect of wall temperature level. However, at high Reynolds number, 75 000 and above, there was about a ten percent spread in the Nusselt number over the wall temperature range, the highest Nusselt numbers being at the lowest wall temperatures. Using a standard film reference temperature, instead of free stream, to compute properties had no influence on this effect. We suspect, but cannot prove, that the flow is in a sensistive transition region with respect to separation, making it temperature sensitive.

It was also noted that there was a tendency for the Nusselt number to level out right at the extreme end of the Reynolds number range. In order to check whether or not this was rig related, a 19.1 mm diameter heater element was installed 180° around the annulus from the 12.7 mm diameter heater and run in a few limited tests. The results are shown in Fig. 6. These data were acquired simultaneously with both the 12.7 and 19.1 mm diameter pins in place. Thus the flow conditions were absolutely identical. From Fig. 6 it is obvious that the leveling off at the high end of the Reynolds number range was a rig phenomenon. It is believed that the flow was choked somewhere in the rig and downstream disturbances no longer fed forward. The turbulence intensity dropped off sharply in this region.

Rotor Wake Data

With the baseline established the rotor was installed in the rig. Flow angle measurements were made with an angle sensitive probe installed in the axial plane of the stator pins. This was 19.1 mm downstream of the rotor. These are shown in Fig. 7. For velocities above 61 m/s, which corresponds to Re = 47 000 in this experiment, the flow angle is less than three degrees for all blade passing frequencies examined. At BPF = 500 Hz the angle is less than

three degrees over the whole range. At the lowest velocities and highest rotor speeds the rotor imparts a tremendous swirl to the flow and makes the data difficult, if not impossible to interpret.

With that as background, Figs. 8 and 9 are typical rotor wake information obtained with a hot wire, located in the plane of the stator. Figure 8 is typical of the hot wire output in the major range of the experiment, where the flow angle was less than three degrees. Figure 8(a) is an instantaneous snapshot of the wake profile as displayed on the FFT analyzer. Only a couple of these instantaneous profiles were recorded; however, the hot wire signal was always displayed on an oscilloscope and Fig. 8(a) is very typical. Figure 8(b) is an ensemble average of the same signal, being triggered by the once/rev signal, for 200 averages. The ordinate on Figs. 8(a) and (b) is voltage. Since the hot wire signal was linearized, this is directly proportional to velocity. However, for two reasons velocity is not shown. First, is the drift problem already discussed. Second, the calibration on the FFT display had a small zero shift problem and did not agree with the digital voltmeters. This in no way impairs the usefulness of these data. The real question is whether or not the circular pin wakes are a good simulation. The profiles in Fig. 8(b) exhibit very good agreement in width, depth and shape with compressor blade wakes presented by Evans (16). The power spectrum showing the fundamental blade passing frequency and many harmonics is also in good agreement with Evans (16). Not surprisingly, there is no spike in the spectra corresponding to the vortex shedding off the stator pins. If it were present, for these conditions and a Strouhal number of 0.25, the frequency would be 1800 Hz. Obviously, the rotor wake overpowers it. Figure 9 is the same information acquired in the flow region where the flow angle is beginning to increase. The very regular wake patterns have disappeared, although the presence of the rotor can still be seen. The flow appears more as a highly turbulent, though somewhat structured, distribution. The heat transfer data in this region will be of little value in rotor wake simulation, however, they may be of some interest in general turbulence effects, and have been included for completeness.

Figures 10 and 11 present the heat transfer and turbulence intensity measurements over the full range of the experiment for the case where the rotor is spaced one stator diameter upstream. The free-stream turbulence with the 3 mesh grid, Fig. 11(b), is 2.5 times the level with the 10 mesh grid, Fig. 10(b). If one were to overlay Figs. 10(a) and 11(a) they would be seen to be absolutely identical, except for the no rotor base cases. Thus, the first observation is that the rotor disturbance completely overpowers the freestream turbulence effect, at least at the relatively low levels of the present experiment. Although there is quite a bit of scatter, the turbulence intensities behind the rotor are similar on both Figs. 10(b) and 11(b). The overall heat transfer increases from 10 to 45 percent depending on the circumstances. Focusing for the moment on the BPF = 500 Hz case, the main observation is that the Nusselt number shifts up above the no rotor case at almost the same slope. It is not appropriate to express it in terms of a percent increase over the no-rotor base case, since the BPF = 500 Hz data are the same for both grids. At the high end of the Reynolds number range the data simply shift to a new level with each increase in speed. Using the BPF = 500 Hz data as a reference, increasing to BPF = 1500 increased Nusselt number about 12 percent and increasing to BPF = 2500 increased Nusselt numbers about 16 percent. At the highest Reynolds numbers the leveling off in the Nusselt numbers was a rig phenomenon, as explained in connection with Fig. 6. At the low end of the Reynolds number range and at the high blade passing frequencies there is a change of slope and a shift up in Nusselt number. This appears to occur in the same range were the discrete wakes breakdown into high turbulence, (see fig. 9).

The data shown in Fig. 12 are a repeat of the conditions of Fig. 10 with the rotor-stator spacing doubled to two stator diameters. All the general trends are the same as with the one stator diameter spacing. The turbulence levels and Nusselt numbers are lower. At BPF = 500 the average turbulence intensities are about 12 percent lower and the corresponding Nusselt numbers are about 12 percent lower. The data are somewhat sparse, because one of the pins broke off of the rotor during these tests and in the process bent all the other pins. Although the pins are being replaced for future experiments, it was not considered necessary to pursue this experiment further.

It has become common (17, 18) to consider the effect of freestream turbulence on stagnation region heat transfer in the following manner.

$$Nu/\sqrt{Re} = f(Tu\sqrt{Re}) \qquad (5)$$

The grouping $Nu/\sqrt{Re}$ is known as the Froessling number and evolves from Froessling's solution of the laminar stagnation region (19). The idea in Eq. (5) is that the "zero turbulence" laminar case is enhanced in some way by the turbulence intensity. The suggested correlation is a power series in $Tu\sqrt{Re}$. Lowery and Vachon (18) have indicated that this approach can be applied to overall cylinder heat transfer, as well as the stagnation region. Lowery and Vachon present the following equation for stagnation point heat transfer.

$$Nu/\sqrt{Re} = 1.01 + 2.624\left[\frac{Tu\sqrt{Re}}{100}\right] - 3.070\left[\frac{Tu\sqrt{Re}}{100}\right]^2 \qquad (6)$$

They plot overall cylinder heat transfer data but do not attempt a correlation over the full range of the $Tu\sqrt{Re}$. All of the data of the present experiment are plotted in this form in Fig. 13. Equation (6) is plotted for reference. Also, the locus of the overall heat transfer data presented by Lowery and Vachon is plotted. The interesting thing is that the general trend in the data is similar to that expressed in Eq. (6). A rough correlation of the data is as follows:

$$Nu/\sqrt{Re} = 0.60 + 3.14\left[\frac{Tu\sqrt{Re}}{100}\right] - 4.90\left[\frac{Tu\sqrt{Re}}{100}\right]^2 \qquad (7)$$

Equation (7) is also shown on Fig. 13. The trend shown by Lowery and Vachon (18) is somewhat different from that of Eq. (7) at low $Tu\sqrt{Re}$. The same is true of the present data. Nevertheless, the fact that both the stagnation point data and the overall heat transfer can be presented by a parabolic equation suggests that it should be fruitful to pursue this relationship with regard to a blade leading edge, since its geometry falls between the extremes of a stagnation line and full cylinder. Since the data of primary interest is the rotor wake data

with flow angles less than three degrees, it might be useful to look only at these data. They are shown in Fig. 14. A curve through the data of Fig. 14 can be expressed by the following equation:

$$Nu/\sqrt{Re} = 0.42 + 4.22\left[\frac{Tu\sqrt{Re}}{100}\right] - 6.59\left[\frac{Tu\sqrt{Re}}{100}\right]^2 \quad (8)$$

One of the interesting features of Eqs. (6) to (8) is that they suggest there is a maximum enhancement in heat transfer due to turbulence. The maximum enhancement over the $Tu\sqrt{Re} = 0$ case due to turbulence along the stagnation line, according to Eq. (6), would be 1.56 and would occur at $Tu\sqrt{Re} = 43$. For overall heat transfer the maximum enhancement, according to Eq. (7), would be 1.84 and would occur at $Tu\sqrt{Re} = 32$. The leading edge geometry should fall between these two cases. These enhancement numbers certainly agree with the range of industrial practice reported by Colladay (1). Using Eq. (8), however the enhancement would be 2.61, also at $Tu\sqrt{Re} = 32$. This seems quite high. The enhancement is quite sensitive to the zero turbulence intercept, which involved a substantial extrapolation of the data on Fig. 14. If this quadratic retationship is to be used for this problem, it will be necessary to acquire some additional data in the low $Tu\sqrt{Re}$ range. Some additional points in the high range to confirm the existence of a maximum would also be valuable.

SUMMARY OF RESULTS

An experimental rig has been developed which simulates the major elements of the flow in the wake of a turbomachinery rotor blade. The flow channel is a 40.6 cm O.D. by 27.1 cm I.D. annulus. The rotor is a spoked wheel of 1.6 mm diameter pins which can be driven over a blade passing frequency range from 200 to 2900 Hz. Extensive wake surveys have been measured with hot wire anemometry. The useful velocity range of the tunnel is dependent on rotor speed. The maximum tunnel velocity is 120 m/sec. At BPF = 2500 Hz the minimum is 60 m/sec. At 1500 Hz the minimum is 37 m/sec. At 500 Hz and below the minimum is 12 m/sec, which is also the minimum tunnel velocity. Below the stated minimums the wakes are irregular and ill-defined and the flow angles exceed three degrees. Provision is made for placing turbulence grids in the inlet and for moving them axially relative to the rotor.

An experiment was performed to scope the influence of these rotor wakes on heat transfer. Heat transfer coefficients, which were both circumferentially and spanwise averaged, were measured on a heated circular cylinder. The 12.7 mm diameter cylinder was part of a stator ring of eight cylinders, located 12.7 mm downstream of the rotor. A base data set taken with the rotor removed agreed well with published literature. In the Reynolds number and blade passing frequency range where the wakes were well defined the rotor produced a turbulence intensity (wake plus free-stream turbulence) of 6 to 10 percent and a corresponding increase in Nusselt number of 30 to 45 percent above the base. In the region of irregular wakes the turbulence intensity was much higher, on the order of 20 to 25 percent, and the Nusselt numbers were twice the no-rotor base value. Doubling the rotor-stator spacing had only a small effect on both average turbulence intensity and Nusselt number.

A rough correlation of all the heat transfer data could be effected by expressing $Nu/\sqrt{Re}$ as a parabolic function of $Tu\sqrt{Re}$. The correlation suggests that the effect of turbulence intensity on heat transfer will attain a maximum.

REFERENCES

1. Colladay, R. S., "Turbine Cooling, "Turbine Design and Application," SP-290, vol. 3, NASA, 1975, pp. 59-101.

2. Kestin, J., "The Effect of Free-Stream Turbulence on Heat Transfer Rates," Advances in Heat Transfer, T. F. Irvine, Jr. and James P. Hartnett, eds., vol. 3, Academic Press, New York, 1966, pp 1-32.

3. Zukauskas, A., "Heat Transfer from Tubes in Crossflow," Advances in Heat Transfer, T. F. Irvine, Jr. and J. P. Hartnett, eds., vol. 8, Academic Press, New York, 1972, pp 93-160.

4. Morkovin, M. V., "On the Question of Instabilities Upstream of Cylindrical Bodies," NASA CR-3231, Illinois Institute of Technology, Chicago, IL, Dec. 1979.

5. Bayley, F. J., and Priddy, W. J., "Effects of Free-Stream Turbulence Intensity and Frequency on Heat Transfer to Turbine Blading," Journal of Engineering for Power, vol. 103, no. 1, Jan. 1981, pp 60-64.

6. Pfeil, H., Herbst, R., and Schroeder, T., "Investigation of the Laminar-Turbulent Transition of Boundary Layers Disturbed by Wakes," ASME Paper 82-GT-124, Apr. 1982.

7. Stockman, N. O., "Potential and Viscous Flow in VTOL, STOL, or CTOL Propulsion System Inlets," NASA TM X-71799, 1975.

8. American Society of Mechanical Engineers Research Committee on Fluid Meters, "Application, Part II of Fluid Meters," 6th ed., 1971, Interim Supplement 19.5 on Instruments and Apparatus, ASME, New York, 1972.

9. Eckert, E. R. G., and Drake, R. M., Heat and Mass Transfer, 2nd ed., McGraw Hill, New York, 1959.

10. Simoneau, R. J., and VanFossen, G. J. Jr., "Effect of Location in an Array on Heat Transfer to a Short Cylinder in Crossflow," Journal of Heat Transfer, to be published.

11. Hilsenrath, J., et al., "Tables of Thermal Properties of Gases," NBS Circular 564, Nov. 1955.

12. Miller, R. L., "ESCORT: A Data Acquistion and Display System to Support Research Testing," NASA TM-78909, 1978.

13. Kline, S. J., and McClintock, F. A., "Describing Uncertainties in Single-Sample Experiments," Mechanical Engineering, vol. 75, no. 1, Jan. 1953, pp. 3-8.

14. Blevins, R. D., Flow-Induced Vibration, Van Nostrand Reinhold, New York, 1977.

15. Kreith, F., Principles of Heat Transfer, 2nd ed., International Textbook Co., Scranton, 1965.

16. Evans, R. L., "Turbulence and Unsteadiness Measurements Downstream of a Moving Blade Row," Journal of Engineering for Power, vol. 97, no. 1, Jan. 1975, pp 131-139.

17. Kestin, J., and Wood, R. T., "The Influence of Turbulence on Mass Transfer from Cylinders," Journal of Heat Transfer, vol. 93, Nov. 1971, pp 321-327.

18. Lowery, G. W., and Vachon, R. I., "The Effect of Turbulence on Heat Transfer from Heated Cylinders," International Journal of Heat and Mass Transfer, vol. 18, no. 11, Nov. 1975, pp 1229-1242.

19. Froessling, N., "Evaporation, Heat Transfer, and Velocity Distribution in Two-Dimensional and Rotationally Symmetrical Laminar Boundary-Layer Flow," NACA TM-1432, 1958.

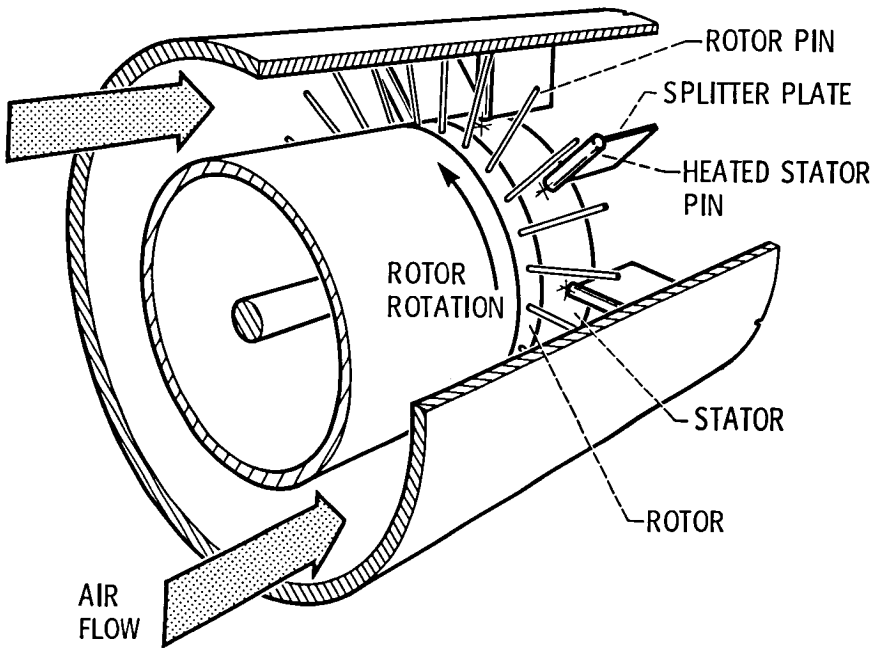

Fig. 1. - Concept of rotor wake heat transfer experiment.

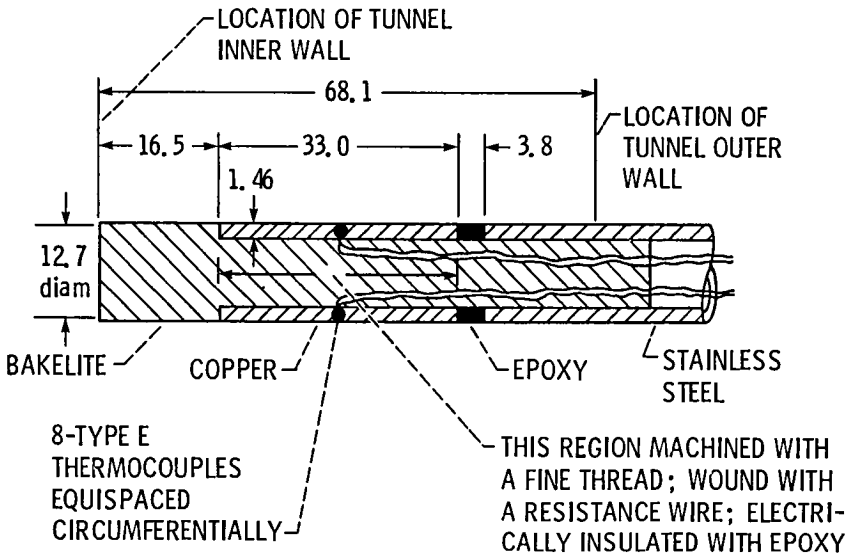

(a) Test section detail.

Fig. 2. - Experimental apparatus for rotor wake heat transfer measurements. (All dimensions in mm.)

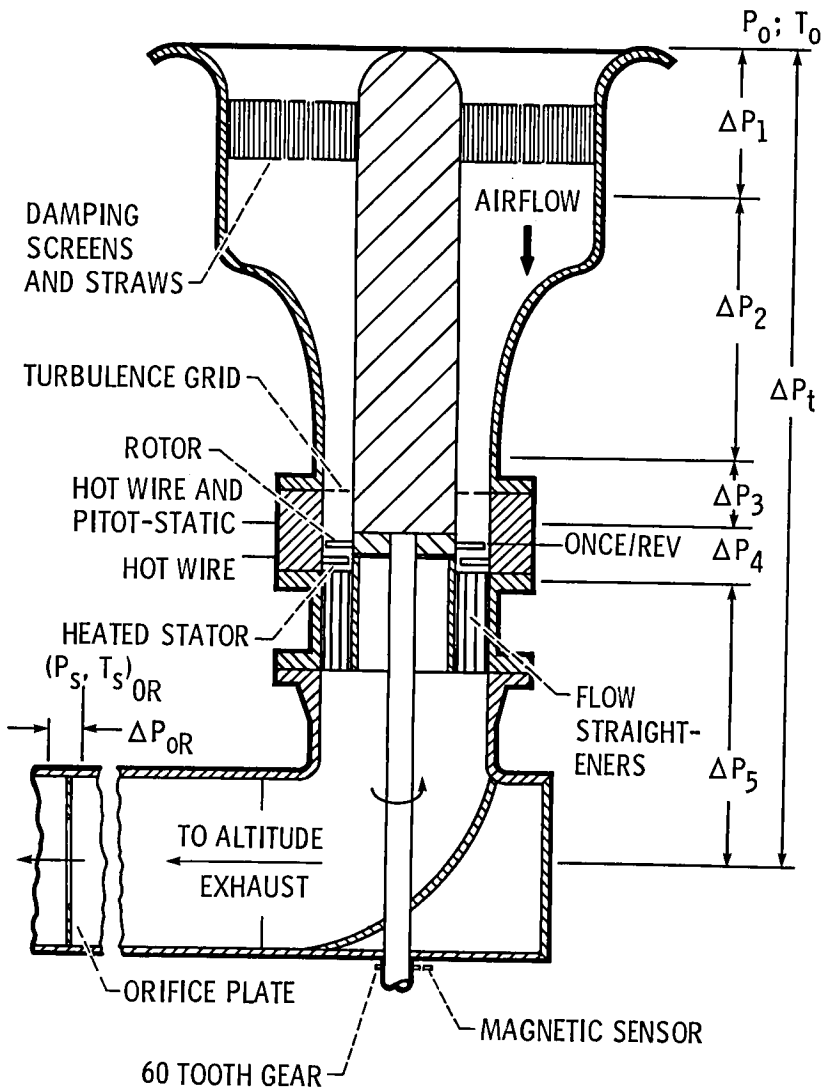

(b) Flow schematic.

Fig. 2. - Concluded.

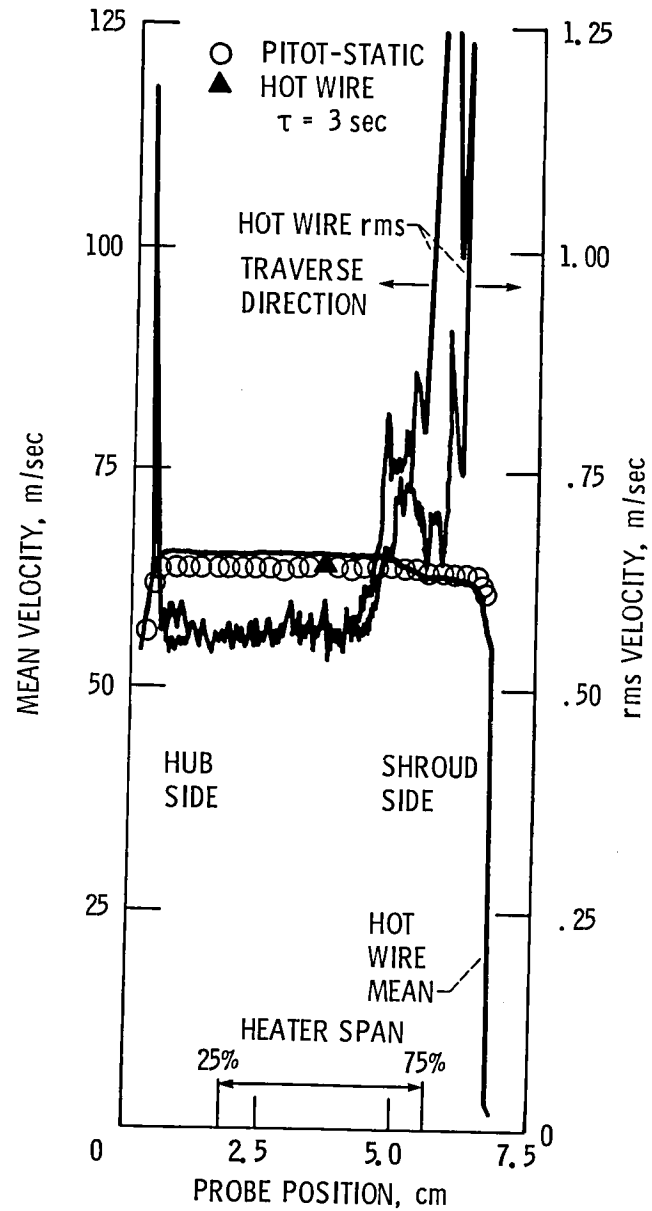

Fig. 3. - Pitot-static, hot wire mean, and hot wire rms velocity profiles surveyed across the inlet. (No turbulence grid.)

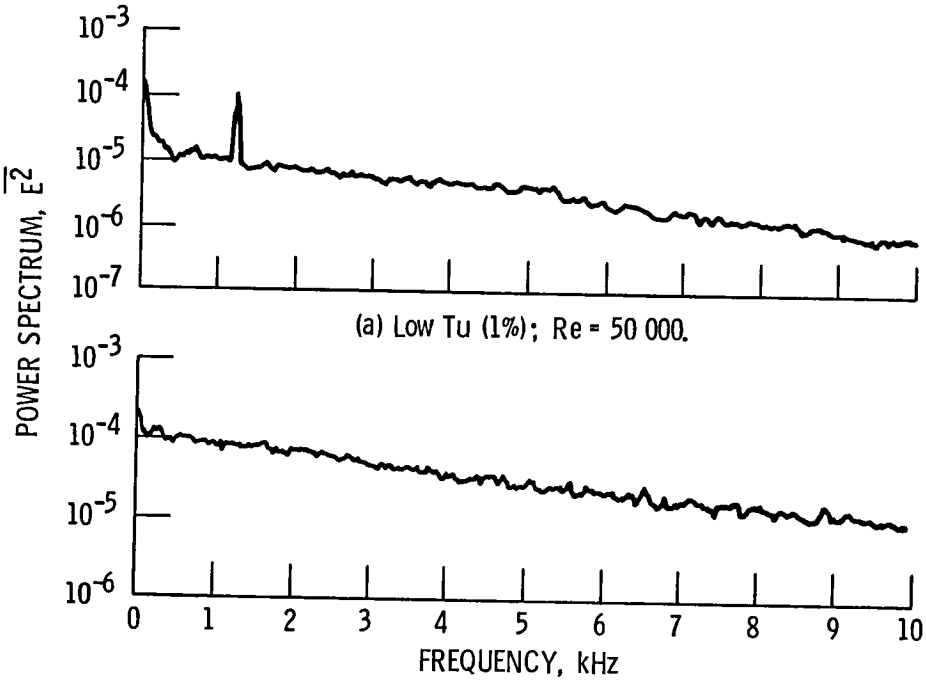

(a) Low Tu (1%); Re = 50 000.

(b) High Tu (4%); Re = 50 000.

Fig. 4. - Spectrum - no rotor.

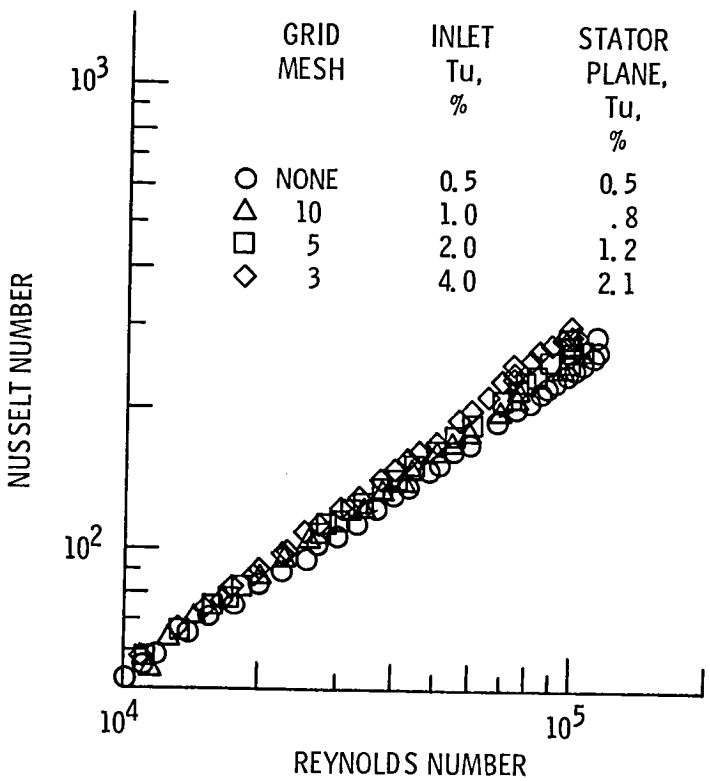

Fig. 5. - Effect of inlet turbulence on heat transfer data - no rotor.

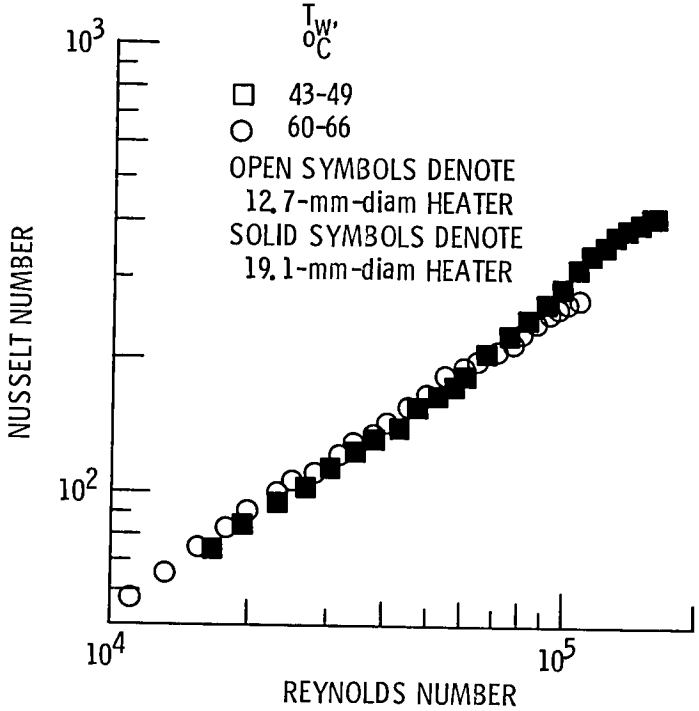

Fig. 6. - Comparison of 12.7 and 19.1-mm-diameter midspan heaters. 8-Pin stator with splitter plates; 5-mesh grid (Tu ≈ 2-3%); no rotor.

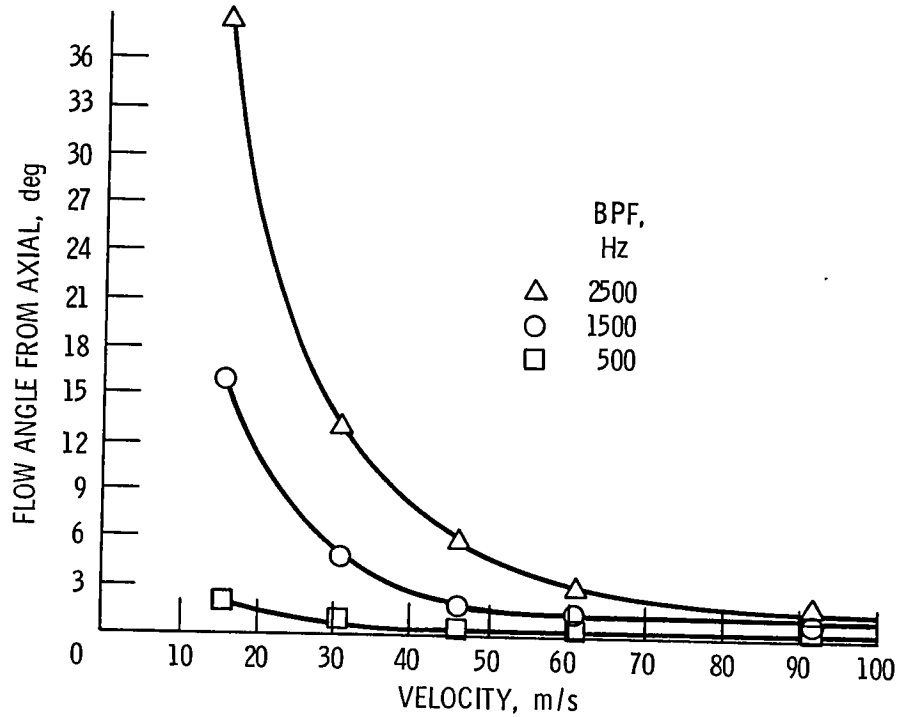

Fig. 7. - Flow angle downstream of rotor as a function of velocity and blade passing frequency.

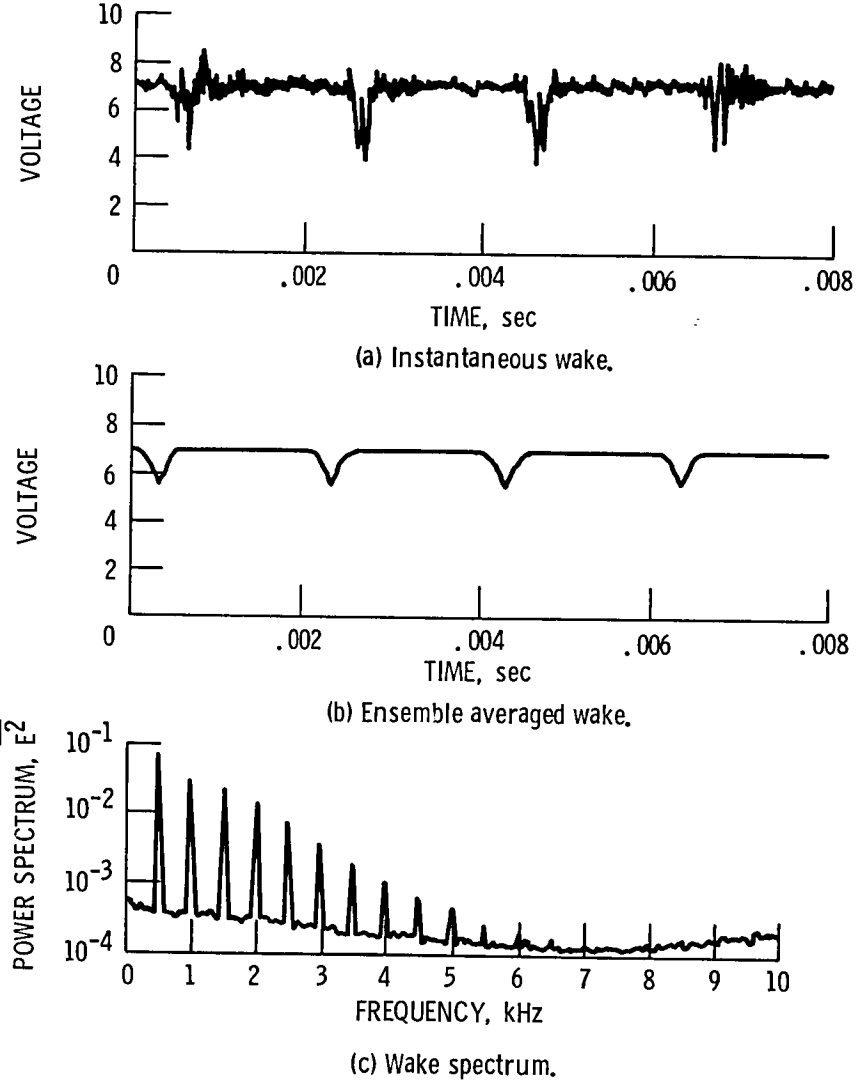

(a) Instantaneous wake.

(b) Ensemble averaged wake.

(c) Wake spectrum.

Fig. 8. - Rotor wake profiles. Re = 70 000; BPF = 500.

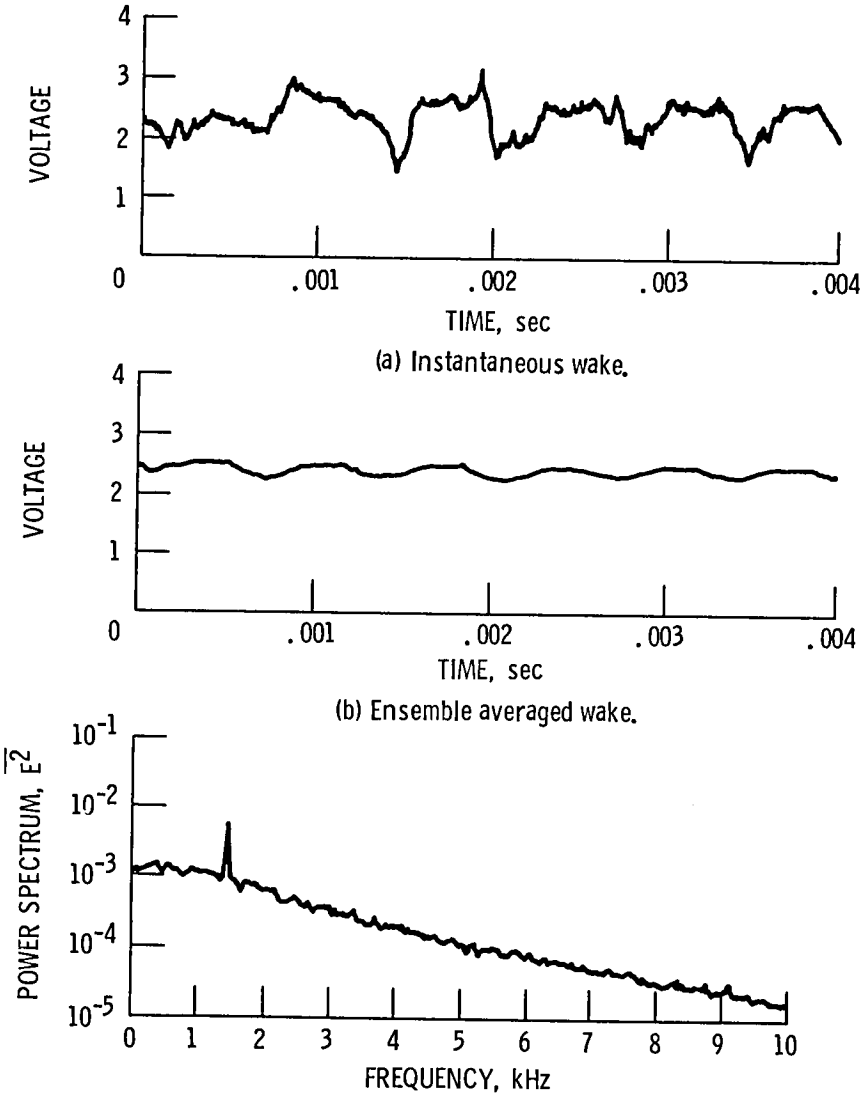

(a) Instantaneous wake.

(b) Ensemble averaged wake.

(c) Wake spectrum.

Fig. 9. - Rotor wake profiles. Re = 20 000; BPF = 1500.

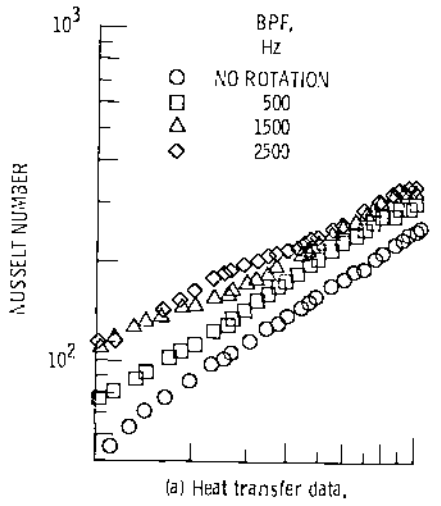

(a) Heat transfer data.

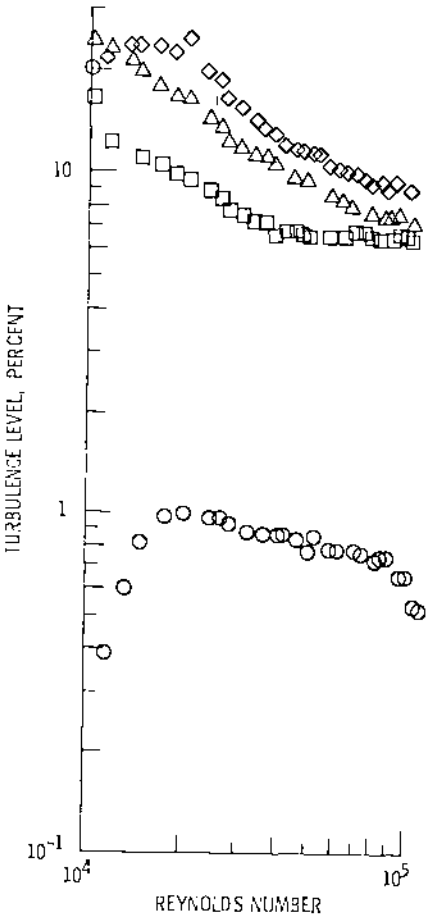

(b) Turbulence levels.

Fig. 10. - Effect of rotor wake on turbulence levels and heat transfer data. Rotor spaced at 1 stator diameter; 10-mesh grid.

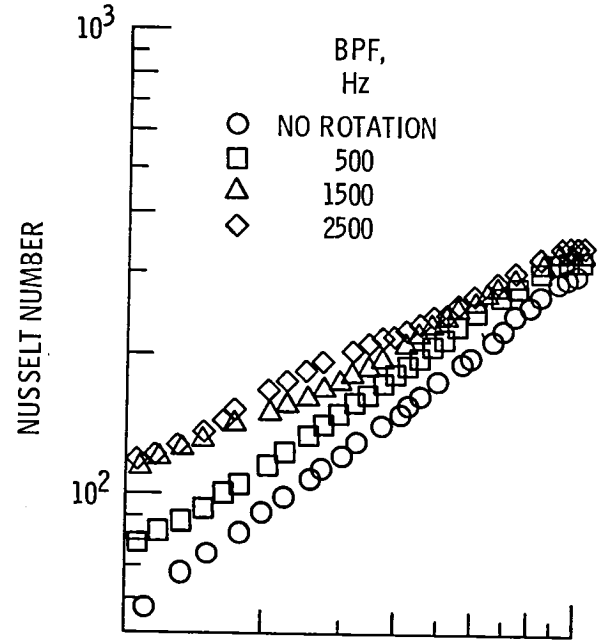

(a) Heat transfer data.

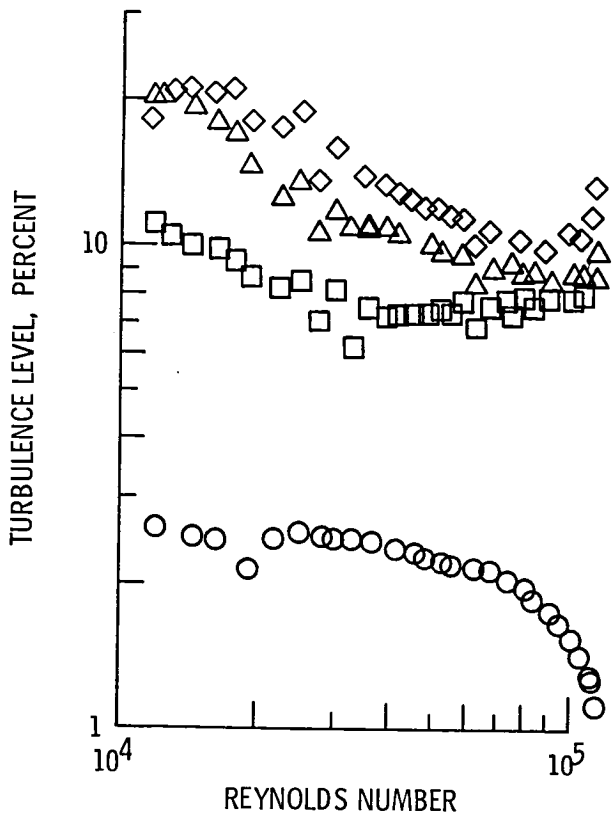

(b) Turbulence levels.

Fig. 11. - Effect of rotor wakes on turbulence levels and heat transfer data. Rotor spaced at 1 stator diameter; 3-mesh grid.

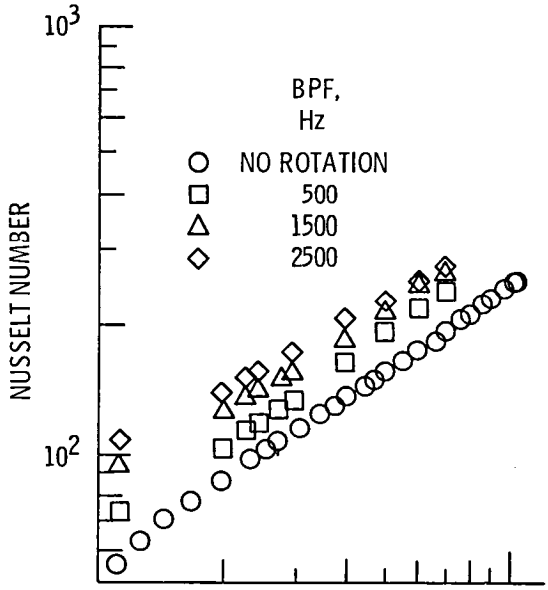

(a) Heat transfer data.

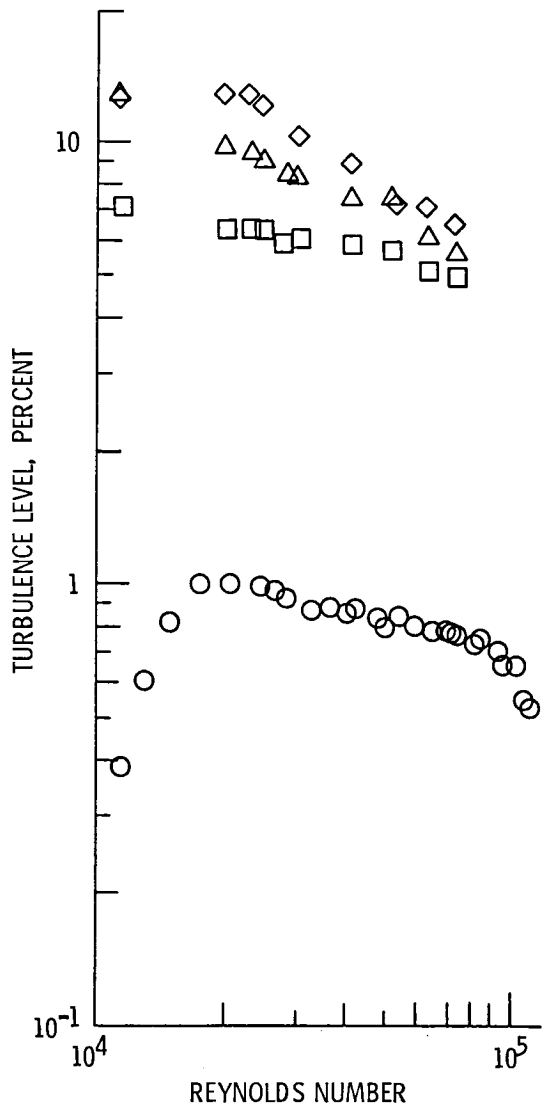

(b) Turbulence levels.

Fig. 12. - Effect of rotor wakes on turbulence levels and heat transfer data. Rotor spaced at 2 stator diameters; 10-mesh grid.

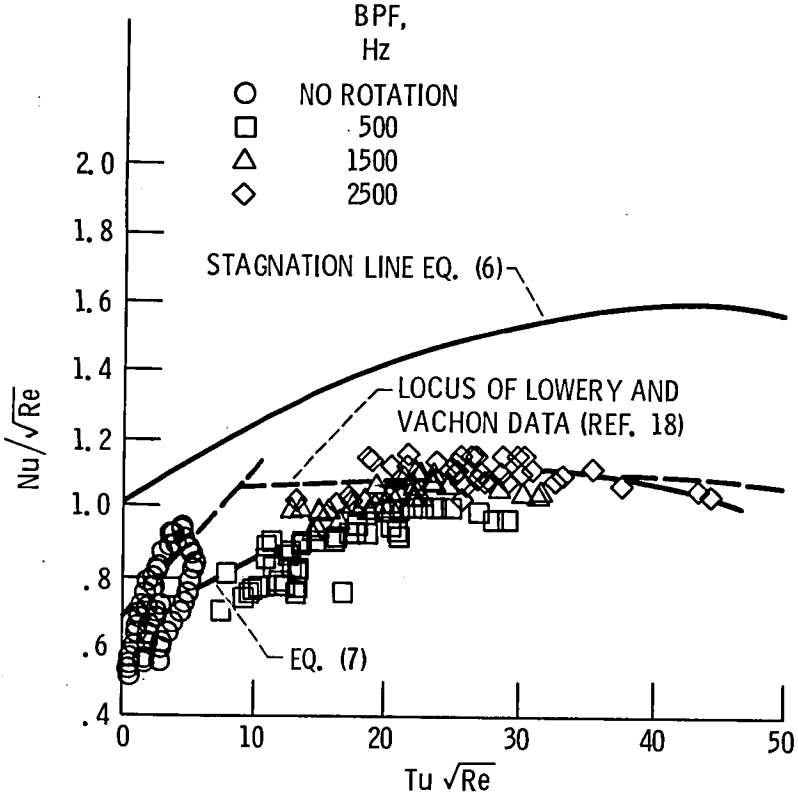

Fig. 13. - Correlation of rotor wake effect in terms of turbulence intensity for all the data of the present experiment, including the no rotation data.

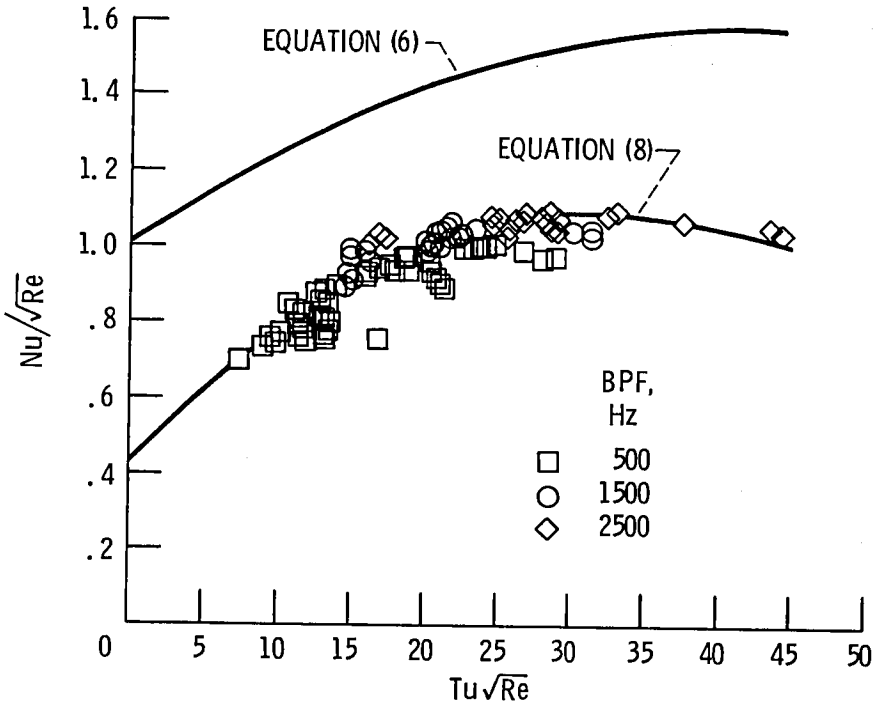

Fig. - 14. - Correlation of rotor wake effect in terms of turbulence intensity for data with flow angles less than 3^{o}.

1. Report No.	2. Government Accession No.	3. Recipient's Catalog No.
NASA TM-83613		

4. Title and Subtitle	5. Report Date
Effect of a Rotor Wake on Heat Transfer from a Circular Cylinder	
	6. Performing Organization Code: 505-31-42

7. Author(s)	8. Performing Organization Report No.
Robert J. Simoneau, Kim A. Morehouse, G. James VanFossen, and Frank P. Behning	E-2039
	10. Work Unit No.

9. Performing Organization Name and Address	11. Contract or Grant No.
National Aeronautics and Space Administration Lewis Research Center Cleveland, Ohio 44135	
	13. Type of Report and Period Covered: Technical Memorandum

12. Sponsoring Agency Name and Address	14. Sponsoring Agency Code
National Aeronautics and Space Administration Washington, D.C. 20546	

15. Supplementary Notes

Prepared for the Twenty-second National Heat Transfer Conference cosponsored by the ASME and AIChE, Niagara Falls, New York, August 5-8, 1984.

16. Abstract

An experiment has been conducted to scope the effect of a rotor wake on heat transfer to a downstream stator. The rotor was modeled with a spoked wheel of 24 circular pins 1.59 mm in diameter. The stator was also modeled with a spoked wheel of 8 circular pins 12.7 mm in diameter. One of the stator pins was electrically heated in the midspan region and circumferentially averaged heat transfer coefficients were obtained. The experiment was run in an annular flow wind tunnel using air at ambient temperature and pressure. Reynolds numbers based on stator cylinder diameter ranged from 10^4 to 10^5. Rotor blade passing frequencies ranged from zero to 2500 Hz. Stationary grids were used to vary the rotor inlet turbulence from one to four percent. The rotor-stator spacings were one and two stator pin diameters. In addition to the heat transfer coefficients, turbulence spectra and ensemble averaged wake profiles were measured. At the higher Reynolds numbers, which is the primary range of interest for turbine heat transfer, the rotor wakes increased Nusselt number from 10 to 45 percent depending on conditions. At lower Reynolds numbers the effect was as much as a factor of two. The rotor wake effect appeared to overpower and wash out the inlet turbulence effect. By treating the rotor wakes as turbulence intensity, a first order correlation could be obtained.

17. Key Words (Suggested by Author(s))	18. Distribution Statement
Heat transfer, Wakes, Turbulence, Cylinders, Turbines	Unclassified - unlimited STAR Category 34

19. Security Classif. (of this report)	20. Security Classif. (of this page)	21. No. of pages	22. Price*
Unclassified	Unclassified		

*For sale by the National Technical Information Service, Springfield, Virginia 22161

National Aeronautics and
Space Administration

Washington, D.C.
20546

Official Business
Penalty for Private Use, $300

SPECIAL FOURTH CLASS MAIL
BOOK

Postage and Fees Paid
National Aeronautics and
Space Administration
NASA-451

NASA

POSTMASTER: If Undeliverable (Section 158
Postal Manual) Do Not Return